PHYSICAL REVIEW D VOLUME 12, NUMBER 9 1 NOVEMBER 1975

Reaction $K^- + p \rightarrow \Lambda + \pi^0$ from 1647 to 1715 MeV*

R. A. Ponte,† S. S. Hertzbach, J. Button-Shafer, and S. S. Yamamoto‡
University of Massachusetts, Amherst, Massachusetts 01002

E. L. Hart
University of Tennessee, Knoxville, Tennessee 37916

R. M. Rice§
University of Tennessee, Knoxville, Tennessee 37916
and University of California, Riverside, California 92502

R. B. Bacastow‖ and S. Y. Fung
University of California, Riverside, California 92502
(Received 26 December 1973)

This paper contains the results of a study of the reaction $K^-p \rightarrow \Lambda\pi^0$ in the center-of-mass-system-energy region of 1647 to 1715 MeV. An energy-dependent partial-wave analysis was performed in this channel. Two allowable solutions were obtained. The first solution in this region contains the D_{13} [$t = 0.08 \pm 0.01$, $\Gamma(E_R) = 44 \pm 11$ MeV, and $E_R = 1671 \pm 3$ MeV] partial wave as the only resonant amplitude; the second solution contains both the P_{11} [$t = 0.16 \pm 0.01$, $\Gamma(E_R) = 81 \pm 10$ MeV, and $E_R = 1671 \pm 2$ MeV] and the D_{13} [$t = 0.17 \pm 0.01$, $\Gamma(E_R) = 76 \pm 5$ MeV, and $E_R = 1655 \pm 2$ MeV] partial wave as resonant.

INTRODUCTION

This paper presents the results of a study of the reaction

$$K^- + p \rightarrow \Lambda + \pi^0$$

in the momentum region 690 to 840 MeV/c. Preliminary results for this channel and the elastic and charge-exchange channels have been reported previously.[1,2]

The range of center-of-mass energies covered is 1647 to 1715 MeV. This energy region, which contains the s-channel resonance $\Sigma(1660)$ in the D_{13} partial wave ($J^P = \frac{3}{2}^-$), has long been marked by discrepancies between production and formation experiments. Until recently, formation experiments[3-7] generally observed only one $I = 1$ hyperon resonance [the $\Sigma(1660)$] in this region. Production experiments, on the other hand, gave evidence for an additional $I = 1$ resonance having a mass of 1690 MeV,[8-13] with a spin-parity assignment of $J^P = \frac{5}{2}^+$ proposed by Sims *et al.*[11] Disconcertingly, several other production experiments[14-16] yielded evidence for the existence of two $\Sigma(1660)$ resonances, degenerate in mass and width and possibly having the same spin and parity, but differing in decay branching ratios and production mechanisms. Additional evidence for this hypothesis is claimed in a partial-wave analysis by a Chicago-Lawrence Berkeley Laboratory (LBL) collaboration.[17] To confuse further the situation in this energy region, evidence has been obtained in a production experiment[18] for the existence of a resonance with a mass of 1642 MeV, which is perhaps the same resonance seen in the production experiment of Crennell[19] and various analyses of formation experiments.[5,20-22] Kim's multichannel K-matrix analysis[22] yielded evidence for a P_{11} resonance at a mass of 1670 MeV with a width of 50 MeV which might correspond to the effect later seen in the same partial wave by Van Horn[23] at a mass of 1668 MeV with a width of 60 MeV.

A resonance in addition to the D_{13} $\Sigma(1660)$ in this energy region is attractive for several reasons. It might well explain discrepancies in the branching ratios between formation and various production experiments. Those experiments[24] done with K^- beams below 2 GeV/c report values for the $\Lambda\pi/\Sigma\pi$ ratio in agreement with formation experiments. On the other hand, higher-momentum production experiments[25] tend to disagree among themselves and with the results of formation experiments. Such a resonance might clarify inconsistencies between predicted SU(3) decay rates[26] for the $\Sigma(1660)$ into the $\Lambda\pi$ channel and experimental results. Furthermore, a P_{11} resonance is particularly attractive since the $S = -1$, $I = 1$ member of the $J^P = \frac{1}{2}^+$ octet containing the $N(1470)$ is still undetected and is expected to be at a mass of 1650 MeV.

For a more comprehensive review of the above, see the "Review of Particle Properties" (pp. 178 - 181) by the Particle Data Group.[27]

The experiment reported here was undertaken in hopes of resolving some of the above ambiguities by measuring the decay rate of the $\Sigma(1600)$ into

TABLE I. Kinematic fits performed.

Hypothesis number	Number of constraints	Process	Input
1	1	$(\bar{K}^0) \rightarrow \pi^+\pi^-$	π^+, π^- measured
2	3	$\bar{K}^0 \rightarrow \pi^+\pi^-$	π^+, π^- measured, $\bar{K}^0$ two-point direction
3	1	$K^-p \rightarrow \bar{K}^0(n)$	$\bar{K}^0$ from 3C decay fit and K^- measured
5	1	$(\Lambda) \rightarrow p\pi^-$	p, π^- measured
6	3	$\Lambda \rightarrow p\pi^-$	p, π^- measured, Λ two-point direction
7	1	$K^-p \rightarrow \Lambda(\pi^0)$	Λ from 3C decay fit and K^- measured

$\Lambda\pi$ and by investigating any additional resonance coupling into $\Lambda\pi$.

EXPERIMENTAL PROCEDURE

Data

The data for this experiment came from a 240 000-picture exposure of the Columbia-Brookhaven 30-in. hydrogen bubble chamber to the Alternating Gradient Synchrotron low-energy separated K^- beam.[28] The experiment was divided into eight runs, with K^- momenta at the center of the chamber equal to 688, 707, 743, 753, 783, 797, 820, and 833 MeV/c. The film corresponding to momenta of 707, 753, 797, and 833 MeV/c was scanned and measured for all topologies at the University of Massachusetts. Approximately 40% of this film was double-scanned to determine scanning efficiencies. The film at the remaining momenta was scanned (30% double-scanned) and measured for disappearing K^- and neutral V^0, two-prongs and three-prongs at the University of California, Riverside.

The following scanning criteria were applied to select a valid V.

(1) The opening angle was greater than 4° in at least one view, and at most one of the two V tracks spiralled (electron-pair discrimination).

(2) There was no clear δ ray which showed that the V was really a $\pi\mu e$ or μe decay.

(3) The V vertex was identifiable in at least two views either from opening angle or from ionization changes.

(4) A V of large opening angle was rejected (as a stray proton-proton scatter having no visible recoil) if both arms were short and heavily ionizing, and there was no origin within 11 cm in real space.

About 20 000 events were processed through geometry and kinematics programs. The kinematic fits attempted are shown in Table I.

The reactions corresponding to a disappearing K^- and a single V^0 are

$$K^- + p \rightarrow \Lambda + \pi^0,$$

$$K^- + p \rightarrow \Sigma^0 + \pi^0, \quad \Sigma^0 \rightarrow \Lambda + \gamma,$$

$$K^- + p \rightarrow \bar{K}^0 + n,$$

$$K^- + p \rightarrow \Lambda + \pi^0 + \text{neutrals},$$

$$K^- + p \rightarrow \Sigma^0 + \pi^0 + \text{neutrals},$$

$$K^- + p \rightarrow \bar{K}^0 + n + \text{neutrals}.$$

A set of criteria for the separation of Λ and $\bar{K}^0$ decays was chosen after a study of χ^2, effective-mass-squared, and missing-mass-squared distributions. The set of criteria was checked by physicists by means of scan-table examination.

The square of the effective mass of the two charged particles forming the V was computed using the measured momenta with the assumption that the positive track was first a pion (effective mass squared called KEMS) and then a proton (effective mass squared called LEMS).

Measured events which had no geometry rejects and made one of the three-constraint (3C) decay fits were subjected to the following tests:

(1) 3C $\chi^2 \leq 12$ for kinematic hypothesis 2(K),

(2) 3C $\chi^2 \leq 12$ for kinematic hypothesis 6(Λ),

(3) 0.223 GeV^2 < KEMS < 0.273 GeV^2,

(4) 1.22 GeV^2 < LEMS < 1.27 GeV^2,

(5) 0.750 GeV^2 < square of the invariant mass recoiling against the $\bar{K}^0$ in kinematic hypothesis 3.

The decay was classified as a $\bar{K}^0$ if the event passed tests 1 and 3, but failed test 4, and as a Λ if the event passed tests 2 and 4, but failed either test 3 or 5. Events which passed test 1

and/or 2, but failed both 3 and 4 were examined on the scan table. Some of these were classified on the basis of range and ionization; some were discarded as not being V decays; and those judged to be poorly measured were submitted for remeasurement along with events in the following categories:

(1) events scanned but not measured;

(2) one or more tracks rejected in geometry reconstruction;

(3) both kinematic hypotheses 2 and 6 ≤ 3 constraints or 3C $\chi^2 > 12$;

(4) tests 1 and 4 passed but 2 and 3 failed, or tests 2 and 3 passed but 1 and 4 failed.

The remeasured events were again classified using the previous criteria or classified on the scan table by physicists.

Corrections and biases

Because of a scanning bias against short decay lengths, the Λ's were required to have a neutral-track length greater than 3 mm (in space) and to decay inside a truncated cone which represents the useful fiducial volume seen in view 2. A weight, W, which compensated for these cuts was computed for each event:

$$W = [\exp(-t_{\min}) - \exp(-t_{\text{pot}})]^{-1},$$

where $t_{\min}$ is the proper time (in units of the Λ mean life) for the Λ to travel the minimum length and t_{pot} is the time at which the Λ would have left the fiducial volume had it not decayed. As shown in Fig. 1, the sum of weights of all events is independent of the Λ cutoff length for any value ≥ 2.5 mm.

For slow Λ's (backward in the $K^- p$ center-of-mass (c.m.) system) the decay protons of the Λ which go backward in the Λ rest frame may have a very short range in the hydrogen bubble chamber and also cause a scanning bias. Events with a proton track length less than 2 mm (in space) were discarded and compensated for by an analytic weighting factor, W', computed for each remaining event as follows:

$$W' = 2/(1 - \cos\theta_{\max}),$$

where

$$\cos\theta_{\max} = \frac{E - E'\gamma_\Lambda}{\gamma_\Lambda \beta_\Lambda p'}.$$

Here E' and p' are the energy and momentum of the Λ decay proton in the Λ rest frame; E is the laboratory energy of a proton which has a range equal to the proton length cutoff; and $\beta_\Lambda (= p_\Lambda/E_\Lambda)$ and $\gamma_\Lambda (= E_\Lambda/m_\Lambda)$ are determined in the laboratory frame (from the Λ momentum p_Λ, total energy E_Λ, and rest mass m_Λ). The sum of the weights of all events is independent of the proton cutoff length as shown in Fig. 2.

The distribution of $\hat{\Lambda} \cdot \hat{p}$ evaluated in the Λ rest frame should be isotropic for any fixed Λ momentum, p_Λ, since there can be no polarization in the production plane. (The unit vector $\hat{\Lambda}$ is along the direction of transformation into the Λ rest frame, and $\hat{p}$ is along the proton momentum in the Λ rest frame.)

A scatter plot (Fig. 3) of $\hat{\Lambda} \cdot \hat{p}$ versus p_Λ shows two regions deviating from isotropy. The first region corresponds to Λ's with low momentum which decay such that $\hat{\Lambda} \cdot \hat{p} \approx -1$. This corresponds to the (corrected) loss for short proton tracks. The other region corresponds to a Λ momentum of about 1 GeV/c and $\hat{\Lambda} \cdot \hat{p} \approx +1$. In this region the π^- in the decay of the Λ is going backward in the Λ c.m. system, and is produced essentially at rest in the laboratory frame. Since many of these events are lost in scanning, the sample was corrected by

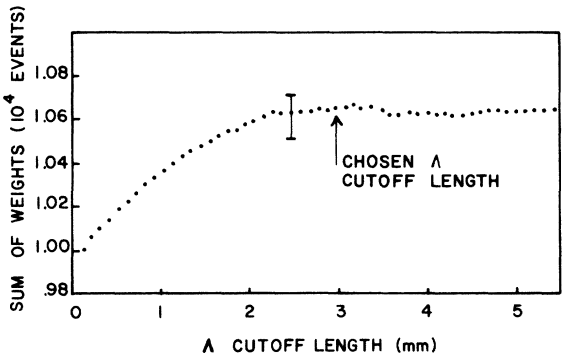

FIG. 1. Weighted number of events as a function of the minimum accepted neutral track length.

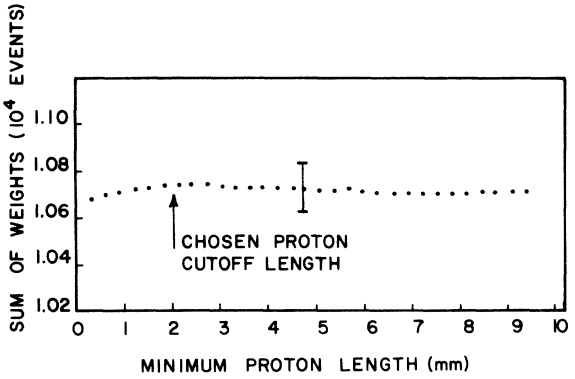

FIG. 2. Weighted number of events as a function of the minimum accepted decay proton track length.

deleting all events with a Λ momentum of 1 GeV/c or greater and with $\hat{\Lambda} \cdot \hat{p} > 0.9$ and weighting the remainder accordingly. This correction affected only a small number of events.

A possible observation bias may occur when the Λ decay plane contains the direction of the observation. The method used to detect this bias was to study the distribution of the azimuthal angle α defined by

$$\cos\alpha = \left| \frac{\hat{z} \cdot (\hat{p}_\Lambda \times \hat{n}_{DK})}{|\hat{z} \times \hat{p}_\Lambda|} \right|, \quad 0^\circ \leq \alpha \leq 90^\circ,$$

where $\hat{z}$ is a unit vector parallel to the optical axis of view 2 and $\hat{n}_{DK}$ is a unit vector normal to the Λ decay plane. A maximum depopulation is expected in the region $\alpha = 0^\circ$. This corresponds to the Λ decay products moving in a plane parallel to the optical axis. A plot of the distribution of α for the sample (Fig. 4) indicated no correction was necessary.

The sample was further corrected for scanning efficiency. The double- and single-scan efficiencies, assuming independent scans, are respectively, given by

$$\epsilon_2 = N_{AB}(N_A + N_B - N_{AB})/N_A N_B,$$

$$\epsilon_1 = 1 - (1 - \epsilon_2)^{1/2}.$$

Here N_A, N_B are the number of events found by scanners A and B, respectively, while N_{AB} is the number found by both scanners.

Taking the last visible bubble as the end of the K^- track introduces errors in fitted Λ production angle and momentum which propagate into the missing mass squared, the quantity used for Λ-Σ separation.

The Λ decay vertex and the Λ momentum from the 1C decay fit (hypothesis 6) were used to calculate the intersection of the Λ path and a straight-line extrapolation of the beam track. The distribution of distances between the measured origin and this intersection point averaged 350 μm (real space). To calculate any systematic error introduced by the decay extrapolation, the procedure was repeated for a topology (2 prong + V°) in which the production vertex was well defined from measurement and the V was a good Λ. The distribution of distance between this intersection point and the measured origin averaged +100μm. Therefore, 250 μm was added to each incident K^- track in all decay fits.

After all previously discussed corrections were made on the data, the Λ lifetime was calculated for a sample of the remaining events using the maximum-likelihood method. The statistical error in the best estimate was calculated using the fact that for very large N the likelihood function becomes Gaussian. The best estimate for the Λ lifetime was $(2.57 \pm 0.03) \times 10^{-10}$ sec for 10 174 events, to be compared with a world average[27] of $(2.578 \pm 0.021) \times 10^{-10}$ sec.

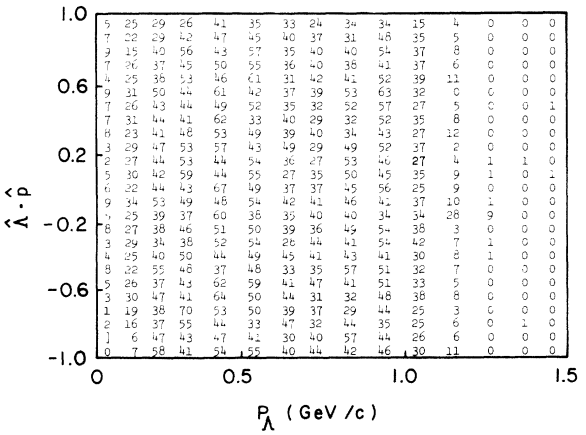

FIG. 3. Scatter diagram of $\hat{\Lambda} \cdot \hat{p}$ versus P_Λ.

ANALYSIS OF DATA

Mathematical form of the angular distribution

The interactions which give rise to a final-state Λ in the zero prong + V topology may be categorized as

$$K^- + p \to \Lambda + \text{neutrals}, \text{ or}$$

$$\to \Sigma^\circ + \text{neutrals}, \quad \Sigma^\circ \to \Lambda + \gamma.$$

The distribution of missing mass squared which would be observed in the reaction $K^- + p \to \Lambda + \text{MM}$ with perfect resolution[29] is shown in Fig. 5. The threshold for $\Lambda\pi^\circ\pi^\circ$ is at $4m_\pi^2$ and the threshold for $\Sigma\pi^\circ\pi^\circ$ is slightly above this.

The problem is to assign events in the sample to different reactions which have final-state Λ's. The most common reactions and their isospins

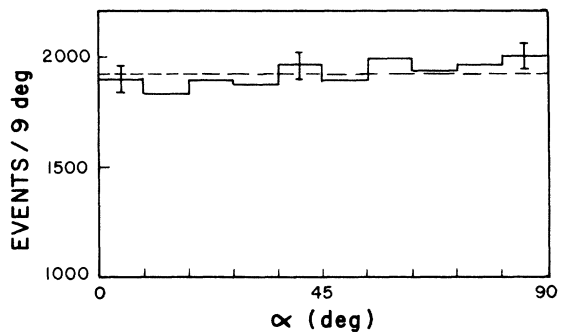

FIG. 4. Distribution of the azimuthal angle α. (See text for definition.)

are

$$K^- + p \to \Lambda\pi^0 \quad (I=1) \quad (1)$$
$$\to \Sigma^0\pi^0 \quad (I=0) \quad (2)$$
$$\to \Lambda\eta \quad (I=0) \quad (3)$$
$$\to \Lambda\pi^0\pi^0 \quad (I=0) \quad (4)$$
$$\to \Sigma^0\pi^0\pi^0 \quad (I=1) \quad (5)$$
$$\to \Lambda\pi^0\pi^0\pi^0 \quad (I=1) \quad (6)$$
$$\to \Sigma^0\pi^0\pi^0\pi^0 \quad (I=0) \quad (7).$$

Although only $\Lambda\pi^0$ and $\Lambda\eta$ offer any kinematical constraints, some information can be obtained considering the missing-mass-squared distribution. Because of experimental resolution the missing-mass-squared plot becomes smeared out. A typical measured distribution is shown in Fig. 6.

A missing-mass-squared cut of $4m_\pi^2$ will eliminate reactions 3 through 7, leaving only reactions 1 and 2. Since $\Sigma^0 \to \Lambda + \gamma$ is unseen, the separation of 1 and 2 can only be accomplished through missing-mass-squared information.

To explain the technique[30,31] used, the following quantities are defined:

$$x = \hat{K} \cdot \hat{M},$$
$$\hat{n} = \hat{K} \times \hat{M} / |\hat{K} \times \hat{M}|,$$

where $\hat{K}$ is the unit vector in the direction of the incident K^-, and $\hat{M}$ is the unit vector in the direction of the missing momentum; both evaluated in the over-all center-of-mass frame of the reaction $K^- + p \to \Lambda +$ missing mass. A study of the experimental resolution function for the missing mass squared (M^2) shows that it approximates a Gaussian for a fixed K^- momentum and x, though the spread $\sigma(x)$ of the Gaussian has a strong functional dependence on x.

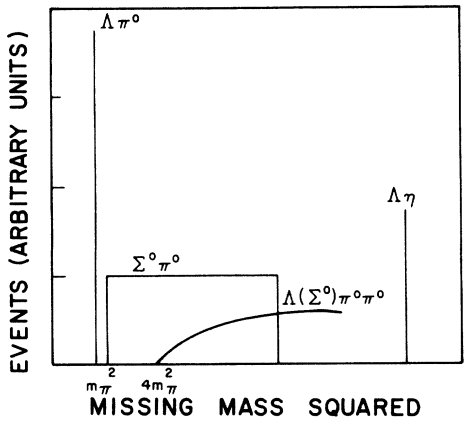

FIG. 5. Distribution of the square of the missing mass from $K^- + p \to \Lambda +$ MM in the case of perfect resolution.

It is important to note that this implies that a fixed missing-mass-squared cut would, in general, include different fractions of $\Lambda\pi^0$ and $\Sigma^0\pi^0$ channels at different angles, thereby distorting the angular distributions.

If the missing-mass-squared distribution for reaction (1) is approximated by a Gaussian about m_π^2 for fixed K^- momentum and each value of x, the distribution function is

$$G_\Lambda(x, M^2) = \frac{1}{(2\pi)^{1/2}\sigma(x)} \times \exp[-(M^2 - m_\pi^2)^2/2\sigma(x)^2].$$

The ideal missing-mass-squared distribution for reaction (2) is uniform between the kinematical limits. [The missing mass squared is given by $m_\Lambda^2 + E_{\text{c.m.}}^2 - 2E_{\text{c.m.}}\gamma_\Sigma(E_\Lambda^{(\Sigma)} + \beta_\Sigma p_\Lambda^{(\Sigma)} \cos\theta_\Lambda^{(\Sigma)})$, where $E_{\text{c.m.}}$ is the total center-of-mass energy; γ_Σ and β_Σ describe the Σ^0 motion as observed in the c.m. frame; and $E_\Lambda^{(\Sigma)}$, $p_\Lambda^{(\Sigma)}$, and $\theta_\Lambda^{(\Sigma)}$ describe the decay Λ in the Σ^0 rest frame. Since the decay is isotropic, this represents a uniform distribution in $\cos\theta_\Lambda$ and hence in the missing mass squared. See Ref. 29, 30, and 32.] The observed distribution is a sum of Gaussians whose centers, M_S^2, are uniformly distributed between the limits, and the distribution function is

$$G_\Sigma(x, M^2) = \frac{1}{N} \int \frac{dM_S^2}{(2\pi)^{1/2}\sigma(x)} \times \exp[-(M^2 - M_S^2)^2/2\sigma(x)^2].$$

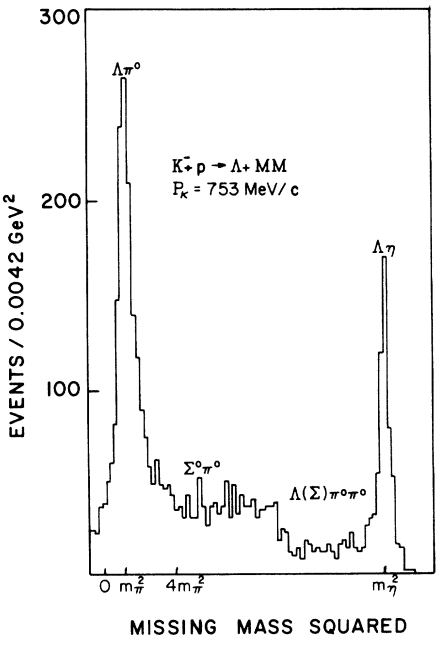

FIG. 6. Distribution of the square of the missing mass from $K^- + p \to \Lambda +$ MM for $P_K = 753$ MeV/c.

Here the limits of integration are the kinematic limits of the uniform distribution and N is a normalization factor.

Therefore, the distribution function describing the angular and missing-mass-squared dependence at production, $f(x, M^2)$, may be expressed as

$$f(x, M^2) = \sum_k [A_k^{\Lambda} P_k(x) G_{\Lambda}(x, M^2) + A_k^{\Sigma} P_k(x) G_{\Sigma}(x, M^2)] = \sum_y \sum_k A_k^y P_k(x) G_y(x, M^2), \quad (8)$$

where A_k^{Λ} are the Legendre expansion coefficients for the $\Lambda\pi^\circ$ angular distribution and A_k^{Σ} are the coefficients for the observed Λ from the $\Sigma^\circ\pi^\circ$ channel. [The differential cross section for either Λ or Σ° would be given by

$$\frac{d\sigma}{d\Omega} = (\lambda\!\!\!^{-2}) \sum_k A_k P_k(\cos\theta).]$$

The method of moments is used to solve Eq. (8). In the limit of large numbers the sample moment (Q_n^y) and the population moment are approximately equal, which implies

$$Q_n^y \equiv \left(\sum_i W_i\right)^{-1} \sum_i W_i G_y(x_i, M_i^2) P_n(x_i) \simeq \int_{x1}^{x2} \int_{-\infty}^{M} f(x, M^2) P_n(x) G_y(x, M^2) dx\, dM^2,$$

where W_i is the "weight" for the ith event (this weight incorporating all of the kinematic, geometric, and scanning losses discussed earlier); $x1$ and $x2$ are, respectively, the minimum and maximum accepted values of the cosine in the production reaction; and M is the cut in missing mass squared which was taken equal to $4m_\pi^2$.

The equation above may be put in the form

$$Q_n^y = \sum_k \sum_{y'} A_k^{y'} C_{nk}^{yy'},$$

where

$$C_{nk}^{yy'} = \int_{x1}^{x2} dx \int_{-\infty}^{M} dM^2 P_n(x) P_k(x) G_y(x, M^2) G_{y'}(x, M^2).$$

From this follows the matrix equation

$$Q \equiv \begin{pmatrix} Q^{\Lambda} \\ Q^{\Sigma} \end{pmatrix} = \begin{pmatrix} C^{\Lambda\Lambda} & C^{\Lambda\Sigma} \\ C^{\Sigma\Lambda} & C^{\Sigma\Sigma} \end{pmatrix} \begin{pmatrix} A^{\Lambda} \\ A^{\Sigma} \end{pmatrix} \equiv CA$$

with solution $A = C^{-1}Q$. The components of Q are the sample moments and the elements of the matrix C are readily calculable once $\sigma(x)$ is determined. The error matrix for the A_k Legendre coefficients was calculated by directly averaging second moments over the data sample of N events:

$$V = (1/N)\langle (A_i - A)(A_i - A)^T \rangle,$$

where A_i is the estimate from an individual event.

The A_k^{Σ} computed by this method may be related to the true $A_k'^{\Sigma}$ through the kinematics of the isotropic $\Sigma^\circ \to \Lambda + \gamma$ decay.[31]

The polarization expansion coefficients are found in a similar manner, where

$$f(x, M^2)\, \vec{P} \cdot \hat{n} = \sum_k \sum_y \alpha_{\Lambda} B_k^y G_y(x, M^2) P_k^1(x)$$

is used to find the first moment of

$$\beta G_y(x, M^2) P_n^1(x).$$

Here $\vec{P}$ is the polarization of the observed Λ, α_{Λ} is the Λ decay-asymmetry parameter, $\beta = \hat{p}_p \cdot \hat{n}$ ($\hat{p}_p$ being a unit vector along the proton direction in the Λ rest frame) and $P_k^1(x)$ is the first-order associated Legendre polynomial. [The polarization is given by

$$P\frac{d\sigma}{d\Omega} = \lambda\!\!\!^{-2} \sum_k B_k P_k^1(\cos\theta).]$$

To obtain an analytic expression for $\sigma(x)$, the mean error ($\mathcal{E}$) in the missing mass squared and its rms deviation ($\Delta\mathcal{E}$) were calculated for each x interval of size 0.2 for $-1 \leq x \leq 1$. The function $\sigma(x)$ was expanded in a power series in x. A least-squares fit was used to find the coefficients of the power-series expansion by seeking the minimum of

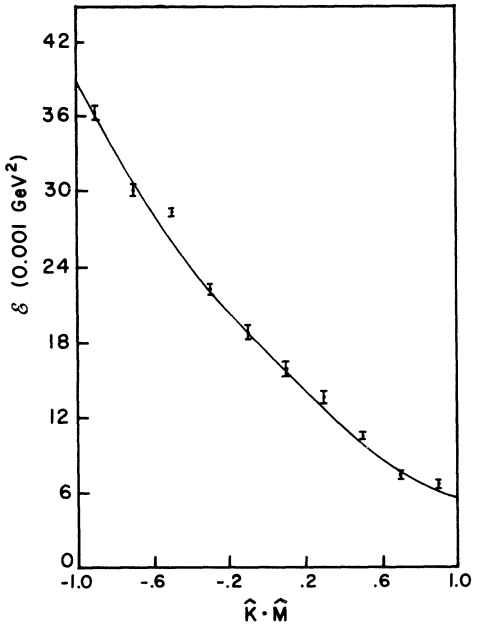

FIG. 7. Resolution in the square of the missing mass as a function of the cosine of the c.m. production angle. The solid curve represents the power series fitted to the empirical values. (See text for details.)

TABLE II. $\bar{K}p \rightarrow \Lambda\pi^0$ Legendre coefficients.

Momentum (MeV/c)	A_1/A_0	$\Delta A_1/A_0$	A_2/A_0	$\Delta A_2/A_0$	A_3/A_0	$\Delta A_3/A_0$	A_4/A_0	$\Delta A_4/A_0$
			Angular-distribution coefficients					
688	0.220	0.107	1.367	0.141	0.621	0.141	−0.026	0.189
707	0.296	0.120	1.226	0.159	0.632	0.160	−0.183	0.216
743	0.276	0.107	1.840	0.146	0.471	0.144	0.651	0.203
753	0.189	0.109	1.722	0.148	0.278	0.148	0.265	0.202
783	0.270	0.116	2.217	0.154	0.716	0.152	0.926	0.212
797	0.265	0.117	2.027	0.153	0.704	0.150	0.667	0.205
820	0.198	0.130	2.219	0.170	0.767	0.166	0.815	0.237
833	−0.246	0.133	1.997	0.176	0.431	0.174	0.622	0.223
Momentum (MeV/c)	$\alpha B_1/A_0$	$\Delta\alpha B_1/A_0$	$\alpha B_2/A_0$	$\Delta\alpha B_2/A_0$	$\alpha B_3/A_0$	$\Delta\alpha B_3/A_0$	$\alpha B_4/A_0$	$\Delta\alpha B_4/A_0$
			Polarization coefficients					
688	0.085	0.100	−0.118	0.103	0.023	0.082	−0.032	0.081
707	−0.065	0.121	−0.190	0.126	0.010	0.102	−0.143	0.096
743	−0.115	0.100	−0.121	0.108	−0.068	0.088	−0.018	0.086
753	0.009	0.104	−0.283	0.113	0.093	0.093	−0.191	0.081
783	−0.106	0.093	−0.181	0.104	0.020	0.084	−0.189	0.083
797	−0.136	0.107	−0.114	0.120	−0.059	0.099	−0.086	0.089
820	−0.221	0.118	−0.009	0.128	−0.029	0.103	−0.096	0.104
833	−0.015	0.130	−0.228	0.135	−0.069	0.115	−0.082	0.097

the χ^2 defined by

$$\chi^2 = \sum_{j=1}^{10} \left[\frac{\sigma(x) - \mathcal{E}_j}{\Delta\mathcal{E}_j}\right]^2 .$$

The power series was truncated on the order of the fit by using χ^2 and an F test. A plot of the power series representing $\sigma(x)$ is given in Fig. 7.

A version of the program SEPAR,[32] was used to calculate the coefficients of the Legendre expansion. Monte Carlo studies were made of the program's ability to discriminate between Σ° and Λ events. Known missing-mass-squared and angular distributions to the same order in Legendre polynomials were Monte Carlo generated for reactions (1) and (2) as input data to SEPAR. When the spread in missing mass squared, $\sigma(x)$, was matched in the Monte Carlo program and SEPAR, misidentification was of the order of 0.5%. Again for matched σ functions, angular distributions were generated such that they corresponded to one nonzero coefficient in the Legendre expansion for Σ°'s and a different nonzero coefficient for the Λ distribution. SEPAR was able to discriminate between Λ's and Σ°'s to the order of 1%. For Legendre coefficients which were zero in the Monte Carlo generating program, SEPAR gave values of 10^{-13} with very large errors. For very poorly matched σ functions, SEPAR misidentification was of the order of 20%. In these cases, SEPAR failed completely to reproduce the experimental angular and missing-mass-squared distributions with a reasonable χ^2.

As a check against possible systematic effects introduced by the σ function for the real sample of events, a missing-mass-squared cut of m_π^2 was applied to the sample. The remaining subsample which contained few Σ°'s was fitted to a Legendre expansion in which no missing-mass-squared information was used. The Legendre coefficients generated from this subsample were compared to the appropriate coefficients generated by SEPAR and no significant difference was found between the two sets of coefficients, though the estimates for the errors of the coefficients were smaller for SEPAR.

Only those events with M^2 less than $4m_\pi^2$ and $-0.9 \leq x \leq 0.9$ were used in generating the final coefficients. This angular interval was chosen to eliminate events which had large poorly determined weights. χ^2's were generated to compare the fit distributions with the sample distributions. χ^2's, F-tests, and the errors on the coefficients were used to determine the order at which the Legendre expansion was truncated. A comparison with coefficients generated without missing-mass-squared information (subsample with M^2 cut of m_π^2; see previous paragraph) showed both methods were in excellent agreement on the order at which the Legendre expansion was truncated. Table II contains ratios of the Legendre coefficients to A_0^Λ for the angular and polarization distributions. The error matrix for these ratios has

TABLE III. Cross section for $K^-p \to \Lambda\pi^0$.

P_K (MeV/c)	$\sigma_{\Lambda\pi^0}$ (mb)
688	3.27 ± 0.23
707	3.18 ± 0.25
743	3.36 ± 0.24
753	3.00 ± 0.22
783	3.85 ± 0.28
797	3.14 ± 0.23
820	3.05 ± 0.24
833	2.72 ± 0.22

large off-diagonal terms varying in size from 20 to 60% of the diagonal terms.

The K^- beam flux was obtained by studying the measured $K^- \to \pi^+\pi^-\pi^-$ decays for the entire exposure. The τ count was used with A_0^Λ from SEPAR to calculate the partial cross section at each momentum (see Table III). These partial cross sections are in good agreement with those reported in various CERN-Heidelberg-Saclay (CHS) experiments[33,34] in the $\Lambda\pi$ channel (see Fig. 8).

Partial-wave analysis

The ratio of the various Legendre coefficients to A_0^Λ and the partial cross section comprised a set of 72 parameters from which the final physics information was obtained by an energy-dependent partial-wave analysis. The connection between the experimentally measured differential cross section (I) and polarization distribution ($I\vec{P}$), and the partial-wave amplitudes $a_{l,J}$ is given by

$$I = |g|^2 + |h|^2,$$

$$I\vec{P}\cdot\hat{n} = 2\mathrm{Re}(g^*h),$$

where

$$g(\theta) = \lambda\bar{} \sum_{l=0}^{\infty} [(l+1)a_{l,l+1/2} + l a_{l,l-1/2}] \times P_l(\cos\theta),$$

$$h(\theta) = i\lambda\bar{} \sum_{l=1}^{\infty} [a_{l,l+1/2} - a_{l,l-1/2}] P_l^1(\cos\theta).$$

Here λ ($\lambda\bar{} = \lambda/2\pi$) is the incoming K^- wavelength evaluated in the K^-p center-of-mass frame. The coefficients connecting the Legendre coefficients A_k^Λ and B_k^Λ to the partial-wave amplitudes $a_{l,J}$ are found in standard tables.[35] With these definitions, the partial cross section is related to the differential cross section by

$$\sigma_{\Lambda\pi} = \int I d\Omega = 4\pi\lambda\bar{}^2 A_0^\Lambda.$$

Resonant amplitudes were parameterized with a Breit-Wigner form

$$T_R^{(l,J)} = \frac{\frac{1}{2}(\Gamma_e\Gamma_r)^{1/2} e^{i\phi}}{(E_R - E) - i\Gamma/2},$$

where E is the c.m. energy, E_R is the mass of the resonance, Γ_e is the partial width in the incident (elastic) channel, Γ_r is the partial width in the final (reaction) channel, and $\Gamma = \sum_i \Gamma_i$, where the summation is over all decay channels of the resonance and ϕ is the phase of the resonant amplitude at resonant energy. [For this experiment

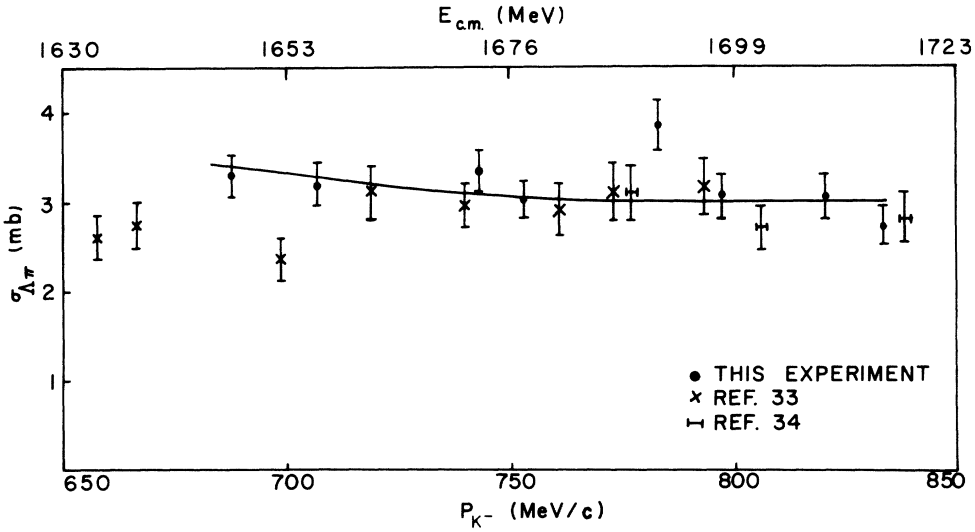

FIG. 8. Cross section for the $\Lambda\pi^0$ channel. The smooth curve is the cross section predicted by the energy-dependent partial-wave analysis.

ϕ is taken to be 0° for the $\Sigma(1660)$ at resonance.]

The width of a resonance is known to have an energy dependence[35] which is, in general, made up of a phase-space factor proportional to k, the relative momentum in the outgoing channel in the c.m. frame, and a centrifugal-barrier factor proportional to $(kr)^{2l}/D_l(kr)$.

Here r is the radius of interaction (taken as 1 F for this experiment). The energy dependence of the width, Γ, used in this experiment was

$$\Gamma(E) = \Gamma(E_R)\left(\frac{k}{k_R}\right)^{2l+1}\frac{D_l(k_R r)}{D_l(kr)},$$

where the $D_l(kr)$ correspond to a square-well potential for nonrelativistic energies.[36] In the fitting procedure the Breit-Wigner form was parameterized as

$$T_R^{(l,J)} = \frac{\pm t}{\epsilon - i},$$

where $t = (\Gamma_e\Gamma_i/\Gamma^2)^{1/2}$ and $\epsilon = 2(E_R - E)/\Gamma$. The parameters varied for a resonant amplitude were t, $\Gamma(E_R)$, and E_R.

Background amplitudes were parameterized as

$$T_B = a + bp_K,$$

where a and b are complex numbers and p_K is the incident K^- momentum in the laboratory frame in GeV/c. In all fits in which background and resonance were present in a given partial wave, the amplitudes were added as

$$a_{l,J} = T_R^{(l,J)} + T_B,$$

where $T_R^{(l,J)}$ is the resonant amplitude for the l, J waves.

By using the ratios A_k^Λ/A_0^Λ and B_k^Λ/A_0^Λ in the fits, the error associated with normalization was restricted to the partial cross section.

The comparison of the experimental Legendre coefficients, A^e and B^e with the calculated coefficients, A^c and B^c is done by computing the minimum of the χ^2 defined by

$$\chi^2 = \sum_{i=1}^{8}\left(\frac{\sigma^e(i) - \sigma^c(i)}{\delta\sigma^e(i)}\right)^2 + \sum_{j=1}^{4}\sum_{k=1}^{4}\left[\left(\frac{A_k^e(i)}{A_0^e(i)} - \frac{A_k^c(i)}{A_0^c(i)}\right)V^{-1}{}_{kj}(i)\left(\frac{A_j^e(i)}{A_0^e(i)} - \frac{A_j^c(i)}{A_0^c(i)}\right) + \left(\frac{B_k^e(i)}{A_0^e(i)} - \frac{B_k^c(i)}{A_0^c(i)}\right)C^{-1}{}_{kj}(i)\left(\frac{B_j^e(i)}{A_0^e(i)} - \frac{B_j^c(i)}{A_0^c(i)}\right)\right],$$

where i represents the various energies, j and k the order of the various Legendre coefficients, and V, C the appropriate error matrices. The full error matrix is employed since the off-diagonal correlation terms of the error matrix, determined experimentally, are fairly large. The significant correlations result from the fact that the set of functions $P_k(x)G_y(x, M^2)$ used to represent the angular distribution were nonorthogonal [see Eq. (8)].

The fitting procedure entails minimization of this χ^2 with respect to each of the parameters. The errors quoted on the various parameters in the fit are obtained from the error matrix H, calculated as the inverse of the second derivative matrix. If $y_1, y_2, \ldots, y_n$ are the variable parameters the error δy_i of a parameter y_i is given by

$$(\delta y_i)^2 = H_{ii},$$

where

$$(H^{-1})_{jk} = \frac{\partial^2\chi^2}{\partial y_j \partial y_k}.$$

The minimization of χ^2 was done using the FORTRAN program MINFUN.[37] After a series of trial runs were made using MINFUN with various parameterizations of partial-wave amplitudes the following assumptions were adopted:

(1) Unitarity was imposed on the amplitudes.

(2) The position of a fitted resonance in a given wave was forced to be between 1597 and 1765 MeV. (This corresponds to ± 50 MeV from the highest and lowest center-of-mass energies available in this experiment.)

(3) For all resonant amplitudes $0 \leq \Gamma(E_R) \leq 200$ MeV.

(4) No background was allowed in a partial wave in which a resonant form was being fitted.

(5) All partial waves which were assumed nonresonant were fitted with background amplitudes.

(6) The D_{13} partial wave was always chosen as resonant.

If any partial wave was chosen to be resonant it was fitted simultaneously with a D_{13} resonant amplitude.

As a reference point a fit was tried with all partial waves fitted to background only; the χ^2 resulting from this was used to determine what further hypotheses were significant. A resonant form was tried in each partial wave and in combinations along with the resonant amplitude in the D_{13} partial wave. All partial waves through F_{15} were tried with a resonant amplitude. Various fits were attempted using the results of Kim's K-matrix analysis[5] for resonances which lie outside the energy range of this experiment, but which are possibly wide enough

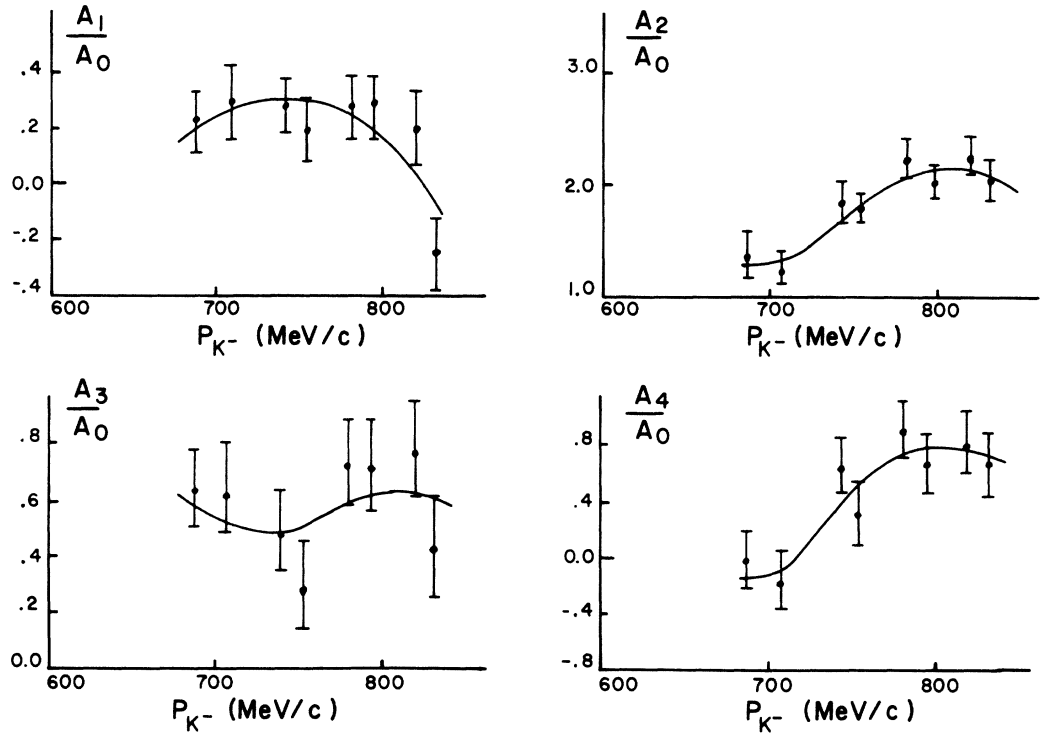

FIG. 9. Experimental results for Legendre-coefficient ratios of the $K^-p \to \Lambda\pi^0$ angular distribution. Curves represent the fit described in Table IV.

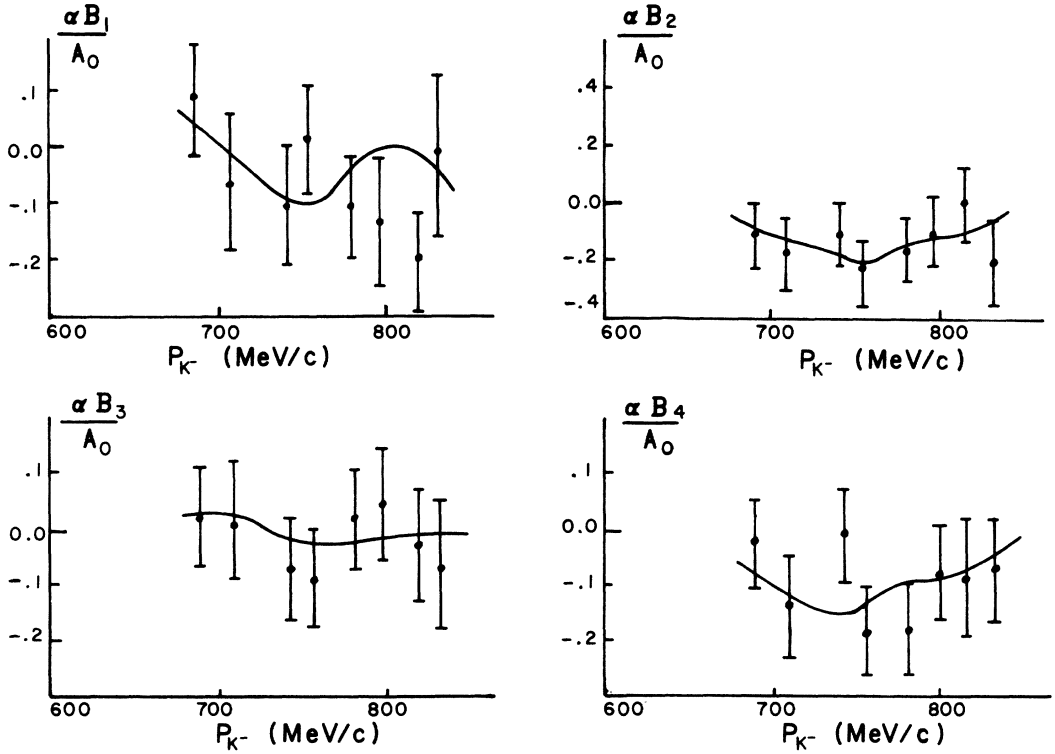

FIG. 10. Experimental results for coefficients of the Λ polarization angular distribution in the $K^-p \to \Lambda\pi^0$ reaction. (The α is the Λ decay-asymmetry parameter.) Curves represent the fit described in Table IV.

TABLE IV. Partial-wave parameters: D_{13} resonant.

Nonresonant amplitudes	Rea	Ima	Reb	Imb
S_{11}	0.21 ± 0.01	0.11 ± 0.01	−0.50 ± 0.01	−0.23 ± 0.01
P_{11}	−0.04 ± 0.01	0.31 ± 0.01	−0.11 ± 0.02	−0.40 ± 0.01
P_{13}	−0.15 ± 0.01	−0.67 ± 0.01	0.23 ± 0.01	0.81 ± 0.01
D_{15}	−0.30 ± 0.01	−0.13 ± 0.01	0.30 ± 0.01	0.20 ± 0.01

Resonant amplitude	Mass, E_R (MeV)	Width, (E_R) (MeV)	Amplitude at resonance, t
D_{13}	1671 ± 3	44 ± 11	0.08 ± 0.01
D_{15}	[1765] [a]	[120]	[−0.25]

[a] [ ] indicates fixed parameters, not fitted.

to affect the fits. Fits in which a fixed resonance [well-established resonance with fixed t, $\Gamma(E_R)$, and E_R] was tried with no background in that partial wave gave large χ^2 or completely unrealistic values for the D_{13} resonance parameters. This led to the conclusion that background should be used in those partial waves in which a fixed resonance was used. The final fitting procedure then entailed trying resonant forms or background in the various partial waves with the D_{13} amplitude treated as resonant.

RESULTS AND CONCLUSIONS

The best fit to the data was obtained for the D_{13} partial wave resonant (without background) and all other waves nonresonant. The χ^2 obtained for this fit was 47 for 53 degrees of freedom, which corresponds to a probability of 70%; the parameters obtained for the D_{13} resonant amplitude were $t = 0.08 \pm 0.01$, $\Gamma(E_R) = 44 \pm 11$ MeV, and $E_R = 1671 \pm 3$ MeV. Figure 8 shows the fitted and experimental cross sections; Figs. 9 and 10 show the fitted and experimental ratios for the Legendre coefficients; and Table IV contains the values of the various parameters obtained for this fit.

The values obtained for the resonance parameters are in good agreement with those obtained in recent CHS experiments which gave $t = 0.10 \pm 0.02$, $\Gamma(E_R) = 50 \pm 10$ MeV, and $E_R = 1660 \pm 10$ MeV. The results are also in agreement with the D_{13} partial-wave parameters from the K-matrix analysis of Kim[22] [$t = 0.07$, $\Gamma(E_R) = 40$ MeV, $E_R = 1670$ MeV]. A comparison of the predicted SU(3) value[23] for the D_{13} amplitude at resonance ($t = 0.05$) is in good agreement with the results of this fit.

As a check of assumption 4 (no background with a fitted resonance) background was added to the Breit-Wigner form of the D_{13} amplitude and a search for a lower minimum χ^2 was attempted. The results gave a poorer confidence level with a probability of 55% for the fit. This indicated the four additional background parameters were not statistically significant. The parameters of the resonance $t = 0.08$, $\Gamma(E_R) = 42$ MeV, and $E_R = 1671$ MeV were not changed much from the fit without D_{13} background.

The analysis of the $\bar{K}N$ channels of this experiment[1] requires the existence of a P_{11} resonance. Kim's K-matrix analysis[22] had indicated the possibility that a resonant P_{11} amplitude at an energy of 1670 MeV is strongly coupled to $\Sigma\pi$ ($x_{\Sigma\pi} = 0.42$) and weakly coupled to $\Lambda\pi$ ($x_{\Lambda\pi} = 0.00$). Several fits were attempted with the D_{13} and P_{11} partial waves resonant, resulting in a best χ^2 of 52 for 54 degrees of freedom which corresponds to a probability of 53%. The parameters obtained for the D_{13} resonant amplitude were $t = 0.17 \pm 0.01$, $\Gamma(E_R) = 76 \pm 5$ MeV, and $E_R = 1655 \pm 2$ MeV; those obtained for the P_{11} resonant amplitude were $t = 0.16 \pm 0.01$, $\Gamma(E_R) = 81 \pm 10$ MeV, and $E_R = 1671 \pm 2$ MeV. Table V contains the values of the various parameters obtained for this fit. Though this is an acceptable solution, the resonant parameters for the D_{13} amplitude are not in good agreement with those from previous experiments.[5,22,23] The amplitude at resonance for the D_{13} partial wave is larger than that observed in most previous experiments, although in agreement with the results of Budgen[7] [$t = 0.165 \pm 0.01$, $\Gamma(E_R) = 59 \pm 4.5$ MeV, $E_R = 1676 \pm 2.0$ MeV]. Furthermore, the width of the D_{13} resonant amplitude is larger than reported in most experiments, though in agreement with the results of Langbein's multichannel analysis[20] [$t = 0.13 \pm 0.03$, $(E_R) = 65 \pm 20$ MeV, $E_R = 1675 \pm 15$ MeV]. This solution indicates that the coupling of a P_{11} resonant

TABLE V. Partial-wave parameters: D_{13} and P_{11} resonant.

Nonresonant amplitudes	Rea	Ima	Reb	Imb
S_{11}	0.01 ± 0.01	0.37 ± 0.01	−0.19 ± 0.01	−0.54 ± 0.01
P_{13}	0.44 ± 0.01	−0.19 ± 0.01	−0.53 ± 0.01	0.39 ± 0.01
D_{15}	0.15 ± 0.01	−0.19 ± 0.01	−0.20 ± 0.01	0.29 ± 0.01

Resonant amplitudes	Mass, E_R (MeV)	Width, $\Gamma(E_R)$ (MeV)	Amplitude at resonance, t
P_{11}	1671 ± 2	81 ± 10	0.16 ± 0.01
D_{13}	1655 ± 2	76 ± 5	0.17 ± 0.01
D_{15}	[1765][a]	[120]	[−0.25]

[a] [ ] indicates fixed parameters, not fitted.

amplitude to the $\Lambda\pi$ channel is much larger than would be expected from Kim's K-matrix analysis[22] [$t = 0.00$, $\Gamma(E_R) = 50$ MeV, $E_R = 1670$ MeV].

A fit was tried with the D_{13} and F_{15} amplitudes as purely resonant and all other partial waves treated as background in order to search for evidence of an F_{15} resonance at 1690 MeV as seen by Sims.[11] Because of the high χ^2 and the fact that the regions of lower χ^2 correspond to very small values of the width [$\Gamma(E_R) \sim 0.02$ MeV] this fit was rejected.

Various individual partial waves (S_{11}, P_{13}, D_{15}) and combinations were tried as resonant, but none gave a satisfactory χ^2 or physically realistic resonant parameters.

Under the assumptions used in this experiment, the data allow two possible solutions for the partial-wave analysis. The first solution contains the D_{13} partial wave as the only resonant amplitude, and the results are consistent with recent analyses as well as SU(3) predictions. The second solution, containing both the D_{13} and P_{11} partial waves as resonant amplitudes, though acceptable, is in disagreement with the results of other analyses.

Two reports have been made of experiments treating just the Λ-plus-neutral final states of low-momentum K^--p interactions. One was carried out with optical spark chambers by Baxter *et al.*[38]; the other was done with a heavy-liquid bubble chamber by London *et al.*[39] Both of these yielded significantly less data than the experiment reported here; and in the latter case, there was no treatment of resonance hypotheses for the $\Lambda\pi^0$ data. Results of these two experiments are consistent with results reported here.

ACKNOWLEDGMENTS

One of us (R. P.) would like to thank Professor R. R. Kofler, Professor E. Golowich, Professor R. G. Carson, and Dr. D. F. Jacobs for informative discussions. We would also like to thank Messrs, J. Chereskie, L. Tokoi, R. Poeton, and J. Roman, and Ms. B. Ruder and H. Winterer for technical assistance, and Ms. D. Lochhead for assistance with computational problems. We are indebted to University of Massachusetts Computing Center for continued cooperation, and gratefully acknowledge a grant of computing time under which some of this work was performed.

*Work supported by the U. S. Atomic Energy Commission.

† Present address: M. I. T. Lincoln Laboratory, Cambridge, Massachusetts 02139.

‡ Present address: University of Tokyo, Tokyo, Japan.

§ Present address: Democritos Nuclear Research Center, Athens, Greece.

‖ Present address: Scripps Institute of Oceanography, LaJolla, California 92037.

[1] R. M. Rice, R. B. Bacastow, S. Y. Fung, E. L. Hart, S. S. Hertzbach, G. W. Meisner, R. Ponte, J. Button-Shafer, S. S. Yamamoto, and D. A. Evans, Bull. Am. Phys. Soc. 15, 1373 (1970); E. L. Hart, R. M. Rice, R. B. Bacastow, S. Y. Fung, S. S. Hertzbach, R. Ponte, J. Button-Shafer, S. S. Yamamoto, and D. A. Evans, in *Baryon Resonances–73*, edited by E. C. Fowler (Purdue University, West Lafayette, Indiana, 1973), p. 311.

[2] R. Ponte, S. S. Hertzbach, G. W. Meisner, J. Button-Shafer, S. S. Yamamoto, E. L. Hart, R. B. Bacastow, S. Y. Fung, and R. M. Rice, Bull. Am. Phys. Soc. 16, 136 (1971).

[3] W. M. Smart, Phys. Rev. 169, 1330 (1968).

[4]D. Berley, E. Hart, D. Rahm, W. Willis, and S. Yamamoto, Phys. Lett. 30B, 430 (1969).
[5]R. Armenteros, R. Baillon, C. Bricman, M. Ferro-Luzzi, E. Pagiola, J. O. Petersen, D. E. Plane, E. Burkhardt, H. Filthuth, E. Kluge, H. Oberlack, in *Proceedings of the 1970 Duke Conference on Hyperon Resonances* (Moore, Durham, North Carolina, 1970), 123; R. Armenteros *et al.*, Nucl. Phys. B21, 15 (1970).
[6]B. Conforto, D. M. Harmsen, T. Lasinski, R. Levi-Setti, M. Raymund, E. Burkhardt, H. Filthuth, S. Klein, H. Oberlack, and H. Schleich, Nucl. Phys. B34, 41 (1971).
[7]D. Budgen, Lett. Nuovo Cimento 2, 85 (1971).
[8]M. Derrick, T. Fields, J. Loken, R. Ammar, R. E. P. Davis, W. Kropac, J. Mott, and F. Schweingruber, Phys. Rev. Lett. 18, 266 (1967).
[9]D. C. Colley, F. Macdonald, B. Musgrave, W. M. R. Blair, I. S. Hughes, R. M. Turnbull, S. J. Goldsack, K. Paler, L. K. Sisterson, W. Blum, W. W. M. Allison, D. H. Locke, L. Lyons, P. J. Finney, C. M. Fisher, and A. M. Segar, Phys. Lett. 24B, 489 (1967).
[10]M. Primer, M. Goldberg, K. Jaeger, V. Barnes, P. Dornan, I. Skillicorn, and J. Leitner, Phys. Rev. Lett. 20, 610 (1968).
[11]W. H. Sims, J. R. Albright, E. B. Brucker, J. T. Dockery, J. E. Lannutti, J. S. O'Neall, B. G. Reynolds, J. H. Bartley, R. M. Dowd, A. F. Greene, J. Schneps, M. Meer, J. Mueller, M. Schneeberger, and S. Wolf, Phys. Rev. Lett. 21, 1413 (1968).
[12]J. Mott, R. Ammar, R. Davis, W. Kropac, D. Slate, B. Werner, S. Dagan, M. Derrick, T. Fields, J. Loken, and F. Schweingruber, Phys. Rev. 177, 1966 (1969).
[13]B. J. Blumenfeld and G. R. Kalbfleisch, Phys. Lett. 29B, 58 (1969).
[14]P. Eberhard, J. H. Friedman, M. Pripstein, and R. R. Ross, Phys. Rev. Lett. 22, 200 (1969).
[15]M. Aguilar-Benitez, V. E. Barnes, D. Bassano, S. U. Chung, R. L. Eisner, E. Flaminio, J. B. Kinson, and N. P. Samios, Phys. Rev. Lett. 25, 58 (1970).
[16]R. D. Estes, J. Duboc, P. H. Eberhard, J. H. Friedman, M. Pripstein, and R. R. Ross, in *Proceedings of the 1970 Duke Conference on Hyperon Resonances* (Moore Publishing Company, Durham, North Carolina, 1970), p. 279.
[17]Chicago-LBL Collaboration, in *Proceedings of the International XVI Conference on High Energy Physics, Chicago-Batavia, Ill.*, edited by J. D. Jackson and A. R. Roberts (NAL, Batavia, Ill., 1973).
[18]A. C. Ammann, A. F. Garfinkel, D. D. Carmony, L. J. Gutay, D. H. Miller, and W. L. Yen, Phys. Rev. Lett. 24, 327 (1970). A. C. Ammann, D. D. Carmony, A. F. Garfinkel, L. J. Gutay, D. H. Miller, and W. L. Yen, Phys. Rev. D 7, 1345 (1973).
[19]D. J. Crennell, W. C. Delaney, E. Flaminio, U. Karshon, K. W. Lai, W. J. Metzger, J. S. O'Neall, J. M. Scarr, A. M. Thorndike, P. Baumel, R. M. Lea, A. Montwill, and T. G. Schumann, Phys. Rev. Lett. 21, 648 (1968).
[20]W. Langbein and F. Wagner, Nucl. Phys. B47, 477 (1972).
[21]N. S. Wong, Nuovo Cimento 2A, 353 (1971).
[22]J. K. Kim, Phys. Rev. Lett. 27, 356 (1971).
[23]A. J. Van Horn, R. P. Ely, and J. Louie, Phys. Rev. D 6, 1275 (1972).
[24]J. Button-Shafer, Phys. Rev. Lett. 21, 1123 (1968); D. O. Huwe, Phys. Rev. 181, 1824 (1969).
[25]For a summary see D. H. Miller, in *Proceedings of 1970 Duke Conference on Hyperon Resonance* (Moore Publishing Company, Durham, North Carolina, 1970), p. 229.
[26]D. E. Plane, P. Baillon, C. Bricman, M. Ferro-Luzzi, J. Meyer, E. Pagiola, N. Schmitz, E. Burkhardt, H. Filthuth, E. Kluge, H. Oberlack, R. Barloutaud, P. Granet, J. Porte, and J. Prevost, Nucl. Phys. B22, 93 (1970).
[27]Particle Data Group, Phys. Lett. 50B, 1 (1974).
[28]D. Berley, Alternating Gradient Synchrotron Division Technical Report No. 258, 1965 (unpublished).
[29]G. Pinski, Nuovo Cimento 24, 719 (1962).
[30]L. Bertanza, A. Bigi, R. Carrara, R. Casali, R. Pazzi, D. Berley, E. L. Hart, D. C. Rahm, W. J. Willis, S. S. Yamamoto, and N. S. Wong, Phys. Rev. 177, 2036 (1969).
[31]D. Berley, S. P. Yamin, R. R. Kofler, A. Mann, G. W. Meisner, S. S. Yamamoto, J. Thompson, and W. Willis, Phys. Rev. D 1, 1996 (1970).
[32]J. Thompson, Ph.D. Dissertation, Yale University, 1969 (unpublished).
[33]R. Armenteros, P. Baillon, C. Bricman, M. Ferro-Luzzi, E. Pagiola, J. O. Petersen, D. E. Plane, N. Schmitz, E. Burkhardt, H. Filthuth, E. Kluge, H. Oberlack, R. R. Ross, R. Barloutaud, P. Granet, J. Meyer, J. P. Porte, and J. Prevost, Nucl. Phys. B21, 15 (1970).
[34]R. Armenteros, M. Ferro-Luzzi, D. W. G. S. Leith, R. Levi-Setti, A. Minsten, R. D. Tripp, H. Filthuth, V. Hepp, E. Kluge, H. Schneider, R. Barloutaud P. Granet, J. Meyer, and J. P. Porte, Nucl. Phys. B8, 233 (1968).
[35]R. D. Tripp, Annu. Rev. Nucl. Sci. 15, 330 (1965); A. Barbaro-Galtieri, in *Advances in Particle Physics*, edited by R. L. Cool and R. E. Marshak (Interscience, New York, 1968), Vol. 2, p. 224.
[36]J. M. Blatt and V. F. Weisskopf, *Theoretical Nuclear Physics*, (Wiley, New York, 1952), p. 361.
[37]A. H. Rosenfeld and W. E. Humphrey, Ann. Rev. Nucl. Sci. 13, 103 (1963).
[38]D. F. Baxter *et al.*, Nucl. Phys. B67, 125 (1973). Bubble-chamber data of the CHS collaboration (R. Armenteros *et al.*, Ref. 5) were combined with the spark-chamber data of this experiment for partial-wave analysis.
[39]G. W. London *et al.*, Nucl. Phys. B85, 289 (1975).